

# INTERNATIONAL SOCIETY FOR SOIL MECHANICS AND GEOTECHNICAL ENGINEERING



*This paper was downloaded from the Online Library of the International Society for Soil Mechanics and Geotechnical Engineering (ISSMGE). The library is available here:*

<https://www.issmge.org/publications/online-library>

*This is an open-access database that archives thousands of papers published under the Auspices of the ISSMGE and maintained by the Innovation and Development Committee of ISSMGE.*

# Research on the Deflexion of Foundations

## Recherches sur la déformation des fondations d'ouvrages

by K. E. YEGOROV, Candidate of Technical Sciences, Academy of Construction and Architecture of the U.S.S.R.  
and

Prof. A. A. NICHIPOROVICH, Doctor of Technical Sciences, Academy of Construction and Architecture of the U.S.S.R.

### Summary

The authors review theoretical and practical investigations on the deflexion of foundation slabs of finite depth, both for industrial and hydraulic structures.

The theoretical investigations include the results obtained by K. E. Yegorov of eccentrically loading a circular stamp founded on an elastic stratum. Formulae have been developed for reaction, tilting and settling, depending on the variation of the ratio of the thickness of the compressed stratum to the radius of the circular stamp. These theoretical investigations should be compared with experimental data of the deflexions of the strata beneath a smokestack foundation of circular form where  $2R = 23$  m. Below the foundation bed, at a depth of 20 m, is debrock which is the incomprehensible part of the foundation bed. In the compressed upper strata, bench marks were placed every 5 m, showing the rapid reduction in deflexion with depth. Measurements have proved that settlement of this foundation is now stabilised.

Investigations of hydraulic structures include measurement of the deflexion of one foundation. This consists of a 200 m stratum of dense clay resting on bedrock. The width of the bed of the structure is 100 m; loads on the soil reach 6 to 8 kg per sq. cm. The forecast of settlements was compared with in-situ observations, which were performed for six years from the time of placing the first lift of concrete. Special attention was directed to several important features influencing deflexion of the foundation bed (heaving of the bottom of the pit, pit flooding, filling of the reservoir, etc.). This foundation is now stable.

### Sommaire

Dans ce rapport, les auteurs présentent les résultats de leurs dernières recherches théoriques et pratiques sur la déformation des couches de fondation d'épaisseur finie à la fois pour les ouvrages industriels et hydrotechniques.

Les recherches théoriques comprennent les résultats obtenus par E. Egorov lors de l'enfoncement d'un plateau rond sous une charge excentrée dans une couche élastique. Sont également données les valeurs de la réaction, des inclinaisons et des tassements en fonction du rapport de l'épaisseur de la couche comprimée au diamètre du cercle chargé. Ces résultats théoriques sont comparés avec les données expérimentales résultant de l'étude de la déformation des différentes couches constituant la base d'appui d'une cheminée ayant une fondation de forme circulaire de  $2R = 23$  m.

Le rocher, incompressible, se trouve à 20 m de profondeur. Des repères de profondeur ont été placés approximativement tous les 5 mètres dans la couche compressible. Ces repères indiquent la décroissance rapide des déformations en profondeur. Actuellement, le tassement de la fondation de la cheminée se trouve stabilisé.

Le rapport donne également des résultats d'études de déformation de la fondation dans le cas d'un ouvrage hydrotechnique. Cette fondation est constituée par une couche d'argile compacte de 200 mètres d'épaisseur recouvrant la roche. La semelle de l'ouvrage a 100 m de large, les charges sur le sol atteignent 6-8 kg/cm<sup>2</sup>. La pression du tassement est comparée avec les données des observations faites sur place pendant les 6 ans qui ont suivi la mise en place de la première couche de béton. Une attention particulière a dû être accordée à une série de particularités influant sur la déformation de la fondation (soulèvement du fond des fouilles, immersion de fouilles, remplissage du réservoir, etc.). Actuellement la déformation de la fondation de cet ouvrage se trouve stabilisée.

## PART I

### Deflexion of foundation of finite thickness

Investigation of the deflexion of strata shows that foundations settle due to the deformation of the upper part of a stratum. Therefore, instead of using an abstract model of a flexible half-space, often employed for design purposes, it is necessary to resort to a more practicable elastic layer model, which can be defined as a model of a foundation of finite depth.

Below are given the results of theoretical and experimental investigations of the deformation of foundation slabs of finite thickness below a circular foundation. For simplifying the theoretical solution of the problem for an elastic stratum under the action of eccentric vertical loads on a circular rigid stamp, it is assumed that there is no friction between the stamp and the soil. Thus, on the upper compressed border of the elastic stratum, the components of normal

stresses  $\sigma_z$  and vertical strain  $w$  are expressed as :

$$\begin{aligned}\sigma_z &= \frac{1}{H} \int_0^\infty \frac{\alpha N(\alpha)}{1-g(\alpha)} \left(\frac{x}{r}\right)^n I_n\left(\frac{r}{H}\alpha\right) d\alpha \\ w &= \frac{2(1-\nu^2)}{E} \int_0^\infty N(\alpha) \left(\frac{x}{r}\right)^n I_n\left(\frac{r}{H}\alpha\right) d\alpha\end{aligned}\quad (1)$$

In equation (1)  $I_n\left(\frac{r}{H}\alpha\right)$  : Bessel function of first type

of  $n$ -th power;  $H$ , thickness of flexible stratum equal to the compressed foundation slab thickness;  $E$  and  $\nu$ , average values of the moduli of deformation and Poisson's ratio for soils within the limits of the compressed thickness. The arrangement of the co-ordinate axes is shown in Fig. 1, where  $x = r \cos \theta$ . The function  $g(\alpha)$  is determined depend-

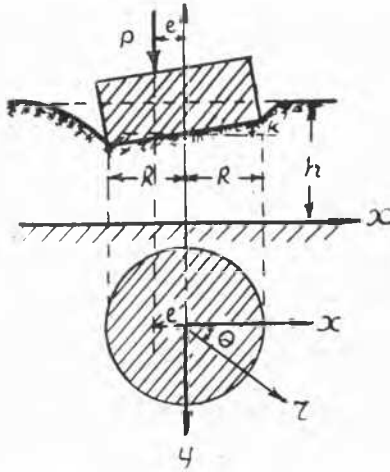


Fig. 1 Eccentric load on circular stamp.  
Charge excentrée sur une fondation circulaire.

ing on the approved border conditions in the plane separating the compressed upper layer of a thickness  $H$  from the unloaded part of the stratum. Assuming that there is no friction in this plane :

$$g(\alpha) = 1 - \frac{\text{Sh}^2 \alpha}{\alpha + \text{Sh} \alpha \text{Ch} \alpha} \quad (2)$$

If it is assumed that the compressed stratum entirely adheres to the unloaded part of the bed, a more complex expression is received for  $g(\alpha)$  :

$$g(\alpha) = 1 - \frac{(3 - 4\nu) \text{Sh} \alpha \text{Ch} \alpha - \alpha}{(3 - 4\nu) \text{Ch}^2 \alpha + \alpha^2 + (1 - 2\nu)^2}$$

For an eccentric load the solution of the problem is in two parts, corresponding to the central load  $P$  and a pair of loads with moment  $M = Pe$ , where  $e$  eccentricity. Equation (1) includes both parts of the problem where the central load, and moment are taken correspondingly with  $n = 0$  and  $n = 1$ .

The unknown coefficient  $N(\alpha)$  is determined from the pair of integral equations (1), taking into account the conditions of the problem. In this case, the radius  $R$  is taken stress  $\sigma_z = 0$  and inside the stamp, in the case of a central load, strain  $w = \text{const}$ , while for a moment acting in the direction of axis  $x$ ,  $w = kx$ , where  $k$  tangent of the angle of turning of the stamp.

For the pair of integral equations (1) the solution at  $n = 0$  corresponding with a central load is given by N. N. LEBEDJEV, J. S. UFLJAND [1], while for  $n = 1$  corresponding with the action of moments is given by K. E. YEGOROV [2]. The final solution of both parts of the problem is reduced to second power Fredholm integral equations, namely :

$$\omega_0(\xi) = 1 + \frac{1}{\pi} \int_0^\infty [K(\eta + \xi) + K(\eta - \xi)] \omega_0(\eta) d\eta \quad (n = 0, 0 \leq \xi \leq 1) \quad (3)$$

$$\omega_1(\xi) = \xi - \frac{1}{\pi} \int_0^\infty [K(\eta + \xi) - K(\eta - \xi)] \omega_1(\eta) d\eta \quad (n = 1, 0 \leq \xi \leq 1) \quad (4)$$

where

$$K(\eta \pm \xi) = \frac{1}{m} \int_0^\infty g(\alpha) \cos \frac{(\eta \pm \xi)\alpha}{m} d\alpha$$

$$\xi = \frac{x}{R}, \quad \eta = \frac{r}{R}, \quad m = \frac{H}{R} \quad (5)$$

Calculations have shown that in order to obtain the required accuracy, it is sufficient to take for functions  $\omega_0(\xi)$  and  $\omega_1(\xi)$  polynomials

$$\omega_0(\xi) = a_0 + a_2 \xi^2 + a_4 \xi^4, \quad \omega_1(\xi) = a_1 \xi + a_3 \xi^3.$$

The values of the coefficients of the polynomials, obtained as a result of solving integral equations (3) and (4) are listed in Table 1. In this case, approximate integral (5) is calculated by means of approximate equation (2) of type [3] :

$$g(\alpha) = 1 - \sum_{i=0}^4 B_i e^{-A_i \alpha}, \quad \text{where } A_0 = 0 \text{ and } B_0 = 1, A_1 = 0.8$$

and  $B_1 = 0.426, A_2 = 1.4$  and  $B_2 = -6.051, A_3 = 2.0$  and  $B_3 = 7.395, A_4 = 2.6$  and  $B_4 = -2.770$ .

In the case of a central load  $P$ , the settlement of a circular footing on a foundation slab, the finite thickness and reactions below are determined by the following formulae :

$$w = \frac{2Rp(1 - \nu^2)}{E} K, \quad p(r) = \frac{C_0 + C_2 \left(\frac{r}{R}\right)^2 + C_4 \left(\frac{r}{R}\right)^4}{A \sqrt{1 - \left(\frac{r}{R}\right)^2}} p \quad \dots (6)$$

Table 1

$m = \frac{H}{R}$	$a_0$	$a_2$	$a_4$	$a_1$	$a_3$
0.2	10.50	-4.90	-1.47	—	—
0.25	8.53	-3.92	-0.90	4.23	-2.33
0.5	4.32	-1.93	0.23	2.14	-0.70
1.0	2.36	-0.54	0.10	1.25	-0.10
1.5	1.78	-0.18	0.02	1.10	-0.03
2.0	1.53	-0.08	0.01	1.04	0
3.0	1.32	-0.02	0	1.01	0
5.0	1.17	0	0	1.00	0
7.0	1.12	0	0	1.00	0
10.0	1.08	0	0	1.00	0
$\infty$	1.00	0	0	1.00	0

where

$$K = \frac{\pi}{4A}, \quad A = a_0 + \frac{1}{3} a_2 + \frac{1}{5} a_4, \quad C_0 = \frac{1}{2} \left( a_0 - a_2 - \frac{1}{3} a_4 \right)$$

$$C_2 = a_2 - \frac{2}{3} a_4, \quad C_4 = \frac{4}{3} a_4, \quad p = \frac{P}{\pi R^2}$$

Where the moment  $M = Pe$  acts, turning of the circular foundation on the slab of finite thickness and the reactions below are determined by the following formulae :

$$\text{tg } k = \frac{(1 - \nu^2)M}{4R^3 EB}, \quad p(r, \theta) = \frac{C_1 \left(\frac{r}{R}\right) + C_3 \left(\frac{r}{R}\right)^3}{B \sqrt{1 - \left(\frac{r}{R}\right)^2}} \frac{ep \cos \theta}{R} \quad (7)$$

where

$$B = \frac{1}{3} a_1 + \frac{1}{5} a_3, \quad C_1 = \frac{1}{2} (a_1 - a_3), \quad C_3 = a_3, \quad p = \frac{P}{\pi R^2}$$

When it is necessary to calculate the reactions only along the line of action of the moment, in equation (7) substitute  $\theta = 0$  and  $r = x$  (Fig. 1). From formulae (6) and (7), it may be concluded that the values of the reactions at the edges of the circular footing equal infinity. This theoretical feature is also met with in the Boussinesq solution for an elastic semi-space. However, at the centre of the round stamp for small values of  $(0 < m \leq 2)$  the reactions increase significantly in comparison with the Boussinesq solution for an elastic semi-space. This aspect significantly lowers the values of the calculated bending moments in slabs and beams on loaded foundations.

For experimental checking of the theory of calculation of foundation bed deformation, the Scientific-Research Institute of Foundations investigated soil deformation in strata under a circular footing ( $R = 11.5$  m) of a smokestack 150 m high [4]. Fig. 2 shows the cross-section of the foundation bed with the depths of the four depth bench marks and physical-mechanical data of soil properties. Diagrams of vertical stresses on the centre line of the foundation are shown. The solid line corresponds to a model of a foundation

of finite thickness at  $m = \frac{H}{R} = 19.5 : 11.5 \approx 2$ . The dotted

line is obtained from an elastic half-space model. In Fig. 3 are shown curves of settlement of foundations and bench marks during an observation period from December, 1957 to May, 1960. The deformation of the upper 5.4 m part of the foundation bed consisting of Quarternary soil deposits equals 70 per cent of the total settlement of the smokestack foundation.

Observations of settlement of the bench marks were started after the foundation had been built, when the load reached 0.6 kg per sq. cm and when the compression of the upper stratum of soil under load was about 10 mm. Settling of bench mark No. 4 installed on the unloaded stratum of limestone was zero. The depth of the limestone stratum below the foundation is 19.5 m. The relative deformation of each of the four foundation strata (Fig. 2) is 0.0093, 0.0025, 0.0013, 0.0011. Lowering of the relative foundation bed deformation with depth is caused mainly by reduction of stress and is partly due to an increase in the modulus of deformation.

In the limits of compressed strata  $H = 19.5$  m at the smokestack foundation bed there are variable soil strata (Fig. 2) with thickness and modulus of deformation correspondingly  $h_1 = 6.3$  m and  $E_1 = 150$  kg per sq. cm,  $h_2 = 3.5$  m and  $E_2 = 200$ ,  $h_3 = 5.5$  m and  $E_3 = 400$ ,  $h_4 = 4.2$  m and  $E_4 = 200$ . Thus, the average value of the modulus of deformation of the compressed strata equals :

$$E = \frac{6.3 \times 150 + 3.5 \times 200 + 5.5 \times 400 + 4.2 \times 200}{6.3 + 3.5 + 5.5 + 4.2} = 240 \text{ kg per sq. cm.}$$

The calculated settlement of the smokestack foundation on a foundation bed of finite thickness is determined by formula (6).

$$W = \frac{2Rp(1 - \nu^2)}{E} \cdot K = \frac{2300 \times 2.8(1 - 0.35^2)}{240} \times 0.47 = 11 \text{ cm.}$$

The value of coefficient  $K = \frac{\pi}{4A} = 0.47$  was calculated for

$m = 19.5:11.5 = 1.7$  by means of Table 1, where the numerical values of  $a_0, a_2, a_4$  are given for equation A. Simulta-

neously, not taking into account that the compressed strata is confined (in case of elastic half-space with  $m = \infty$ ,  $K = \frac{\pi}{4} = 0.79$ ), the calculated settlement of the smokestack

foundation will be greatly exceeded and equals  $W = 18.5$  cm.

In May, 1960, the measured total average settlement of the smokestack foundation was 7.5 cm. Due to the continuing low accumulation of settlement its value after complete stabilization should be near the calculated value of 11 cm.

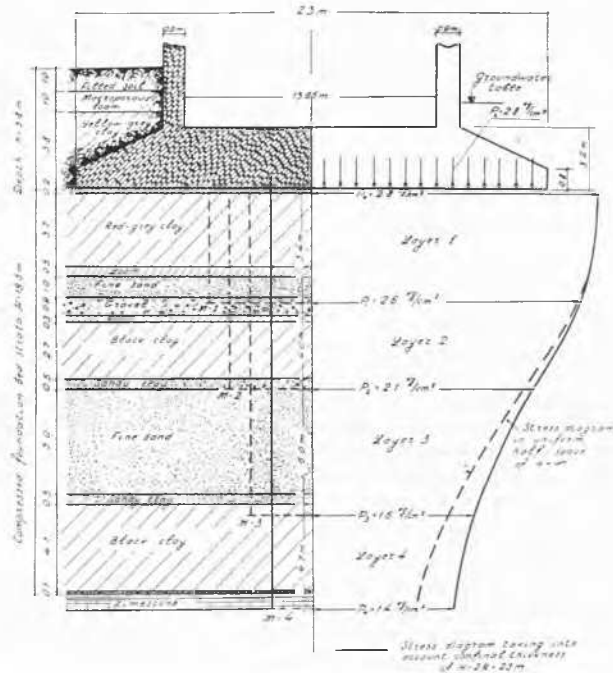


Fig. 2 Vertical cross-section of smokestack foundation bed.

Layer 1 (clay) : volume weight  $\gamma = 1.92$  tons per cu. m; moisture content  $W = 29$  per cent; plastic limit  $W_p = 22$  per cent; liquid limit  $W_L = 58$  per cent; porosity  $n = 46$  per cent; void ratio  $e = 0.858$ ; degree of moisture content  $S = 0.93$ ; modulus of deformation  $E = 150$  kg per sq. cm.

Layer 2 (clay) :  $\gamma = 1.75$  tons per cu. m;  $W = 29$  per cent,  $W_p = 28$  per cent,  $W_L = 53$  per cent,  $n = 41$  per cent,  $e = 0.694$ ,  $S = 0.95$ ,  $E = 200$  kg per sq. cm; ignition losses due to coal content — 35 per cent.

Layer 3 (dense fine sand) :  $E = 400$  kg per sq. cm.

Layer 4 (clay) :  $\gamma = 1.92$  tons per cu. m;  $W = 22$  per cent,  $W_p = 16$  per cent,  $W_L = 29$  per cent,  $n = 39$  per cent,  $e = 0.655$ ,  $S = 0.89$ ,  $E = 200$ ; ignition losses due to coal content — 10 per cent.

Coupe verticale de la fondation de la cheminée :

1<sup>re</sup> couche (argile) : poids spécifique  $\gamma = 1.92$  t/m<sup>3</sup>, humidité  $W = 29$  pour cent; limite de plasticité  $W_p = 22$  pour cent, limite de liquidité  $W_L = 58$  pour cent, teneur en eau  $n = 46$  pour cent, coefficient de porosité  $e = 0.858$ , degré de saturation  $S = 0.93$ , module de déformation  $E = 150$  kg/cm<sup>2</sup>.

2<sup>e</sup> couche (argile) :  $\gamma = 1.75$  t/m<sup>3</sup>;  $W = 29$  pour cent;  $W_p = 28$  pour cent,  $W_L = 53$  pour cent,  $n = 41$  pour cent,  $e = 0.694$ ,  $S = 0.95$ ,  $E = 200$  kg/cm<sup>2</sup> avec 35 pour cent de perte au cours de la calcination du fait de la teneur en matières organiques.

3<sup>e</sup> couche (sable à grains fins compacts) :  $E = 400$  kg/cm<sup>2</sup>.

4<sup>e</sup> couche (argile) :  $\gamma = 1.92$  t/m<sup>3</sup>;  $W = 22$  pour cent,  $W_p = 16$  pour cent;  $W_L = 29$  pour cent;  $n = 39$  p. cent;  $e = 0.655$ ;  $S = 0.89$ ;  $E = 200$ , avec 10 pour cent de perte au cours de la calcination du fait de la teneur en matières organiques.

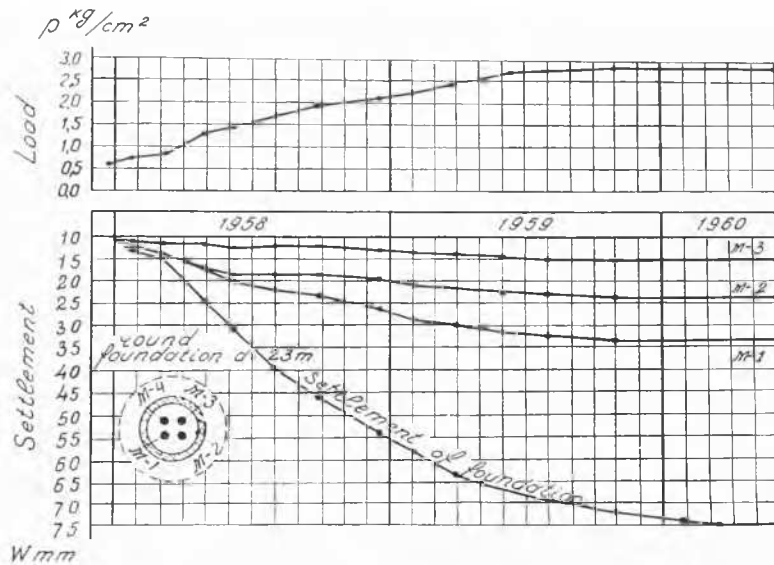


Fig. 3 Graphs of foundation settlement related to bench marks.  
Graphique des tassements de la fondation et des repères en profondeur.

Thus, according to a finite thickness foundation bed mode (elastic layer) the calculated settling of the smokestack foundation is obtained nearer the actual value than by calculations with a foundation bed model in the form of an infinite half-space (elastic half-space).

### Conclusions

Further investigation of foundation bed deformations in layers should corroborate that foundation settlement proceeds mainly by compression of soil directly below the foundations. Thus, any foundation bed may be divided into two parts, consisting of the upper compressed strata and lower unloaded part of the foundation slab. For calculation of foundation bed deformations, the best method is a scheme with an elastic layer over the unloaded foundation bed. The above-mentioned example of investigation of smokestack foundation deformation is typical for the elastic layer scheme, as in the limits of the compressed strata are rocky soils such as limestones. However, if there are no rocky soils at shallow depth, the thickness of the compressed strata should be known, depending on the conditions of the foundation bed, external loads and size of the foundations.

Due to the lack of sufficient experimental data on investigation of foundation bed deformations, the Soviet Standards and Specifications [5] recommend that the thickness of the compressed strata should be calculated on the basis of the ratio between stress in the foundation bed due to the soil weight and those due to the external load.

## PART II

### Design and actual settlement of power house on dense clay

The authors give measurements of actual settlement of a large power station, comparing these measurement with the design forecasts\*.

The cross-section of the proposed hydroelectric station is given in Fig. 4 (a). The power house itself, where the tur-

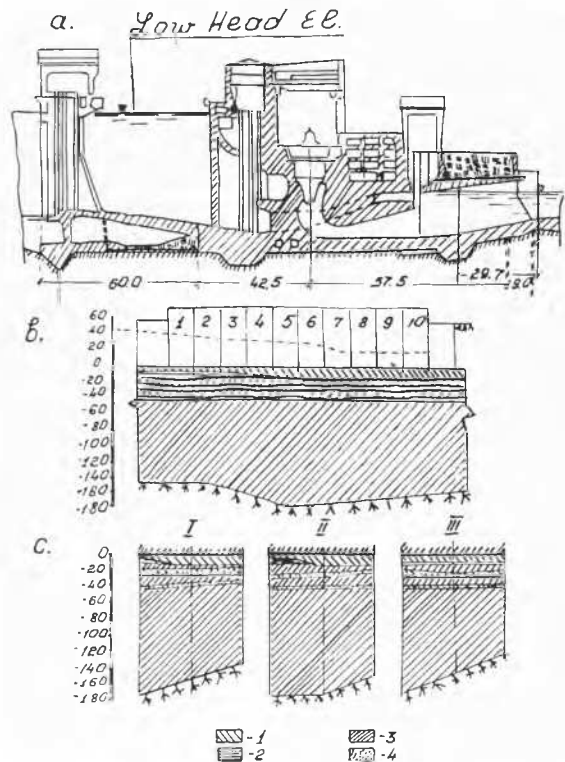


Fig. 4 (a) Cross-section of hydroelectric station.  
(b) Longitudinal geological section.  
(c) Geological cross-sections.  
(a) Coupe transversale de l'usine hydroélectrique.  
(b) Profil géologique longitudinal.  
(c) Profil géologique transversal.

\* This was undertaken by a team of scientific workers of the Hydro-technical Laboratory of the *Vodgeo Institute* consisting of Junior Scientific Workers T. I. Tzibulnik, V. M. Pavilonsky and V. I. Rylejev under the guidance and collatoration of Prof. A. A. Nichiporovich. Data on in-situ observations were obtained in the Scientific-Research Sector of *Gidro project*.

bines, draft tubes and generators are placed, is about 75 m high, the width of the foundation being about 100 m. Longitudinally, the power house is about 600 m long, all structures being cut by temperature joints into 10 blocks, each of them having two sets.

The upstream part of this scheme is an anchored portion of the spillway, at the beginning of which is a trash rack. At the downstream face, a stilling apron has been provided at the power station consisting of concrete slabs with a maximum thickness of 6 m.

Horizontally, the proposed hydroelectric station has its right abutment (section 1) adjoining the bank through the mounting bay, while the left (section 10) through a semi-abutment and wings adjoins an earth dam.

The foundation of the power house, both longitudinally and transversely, consists of a thick layer of clay, comprising Quarternary alluvial-talus deposits at the top, and at the bottom bedrock deposits of the newer and older Pliocene. Bedrock is at a depth of about 175 m. The results of many geological investigations were used to forecast the foundation settlement.

Lithologically, the entire strata is variable and the geologists divided it into several (up to 14) layers. The analysis of geological features permitted these to be greatly reduced in number, some being amalgamated.

The final schematic geological sections at three design stations (sections 1-5 and 10) are shown in Figs. 4 (b) and 4 (c).

The design characteristics of individual features were obtained by statistical treatment of the results of compression tests performed with water-immersed samples. The tests proved that the bedrock clay swells when moistened.

The dilation index is the value of  $P_a$ , called the dilative capacity\*.

Special investigation of dilatation of similar soils determined the links between values  $P_a$  and the total dilatation of the sample  $\theta$  per cent as well as the nature of changing of the void ratio  $e = f(P)$  in the range of length  $P_a$  during dilatation of the sample under a load less than  $P_a$ .

The compressed soil strata were divided into two zones the dilatation zone of a depth of  $h_p$ , and the undisturbed zone  $h_H$ . The dilatation zone was determined by equation (4).

$$h_p = \frac{P_{a \text{ av}}}{\gamma}$$

where  $P_{a \text{ av}}$  — average of values  $P_a$  in the considered layer. For this approach it was found that  $h_p = 30$  m.

When determining the design loads on the foundation, it was assumed that the trench would be flooded for a long period before construction was completed. For these conditions, the maximum load on the foundation is the load of the structure during the period of operation (Fig. 5 (a)) —  $P_{oper}$ , which is taken as the design value in the dilatation zone.

However, in the undisturbed zone, the design load is determined by formula  $P_{des} = P_{oper} - P_{pit}$ , where  $P_{pit}$  — load equal to weight of soil excavated from trench.

Determination of stresses and calculation of the probable settlement were performed by the usual methods, based on the theory of elasticity.

Design calculations were done for fifteen alternative proposals with variations of the following factors: rigidity of foundation, trench width, soil properties and others, showed a considerable influence on the final results of calculating design loads, determination of zones and estimation of foundation bed dilatation, specification of design soil properties and several other factors which are often not taken into account when forecasting settlement.

The final calculation method was selected after detailed analysis of all results and their comparison with empirical functions derived from actual settlement observations on

\*  $P_a$ -horizontal length of the compression curve, obtained when resistance is created preventing dilatation of the soil in the consolidometer.

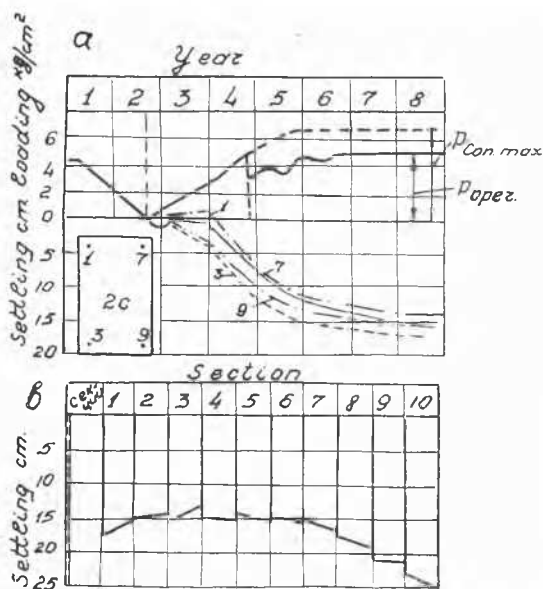


Fig. 5 (a) Changing of loads and settlement with time at section 2.

(b) Settlement of section at six years after start of concreting.

(a) Modification des charges et tassements suivant le temps sur la section n° 2.

(b) Tassements de la section, à la sixième année après le coulage.

several large hydraulic structures [6, 7]. The recommended values for average settlement before erection of three stations are given in Table 2.

Table 2

Station No.	Design data (in cm)				Site data
	Final settlement		Settlement at end of construction period		
	$W_{\infty I}$	$W_{\infty II}$	$W_{con I}$	$W_{con II}$	$X_{con in-situ}$
I (10c)	48.0	26.2	33.6	18.3	19.7
II (5c)	45.0	18.6	31.5	13.0	13.8
III (1C)	45.0	19.0	31.5	13.3	13.8

By employing the results of in-situ observations during the initial period of construction, the values of the possible final settlement were determined accurately.

On this basis, after obtaining a more precise forecast, the values of the final settlement of the second order —  $W_{\infty II}$ , as listed in Table 2, were determined.

Settlement at the end of the construction period is a factor of great importance. It has also been determined by an empirical equation based on in-situ observations of 16 similar structures [6, 7].

According to this function, for the proposed project  $W_{con} = 0.7W_{\infty}$ .

Thus, the values of  $W_{con I}$  and  $W_{con II}$  were obtained and these are also listed in Table 2.

The in-situ observations of foundation bed soil deformations of the proposed project were started a long time before concrete placing began by means of bench marks embedded at different elevations in the foundation bed.

The depth of the dilatation zone, according to the data of these measurements, is about 30 m. After excavating the trenches for separate sections and concrete placing, observations began of the deformation of the concrete blocks by bench marks embedded in the concrete blocks and transferred to higher elevations as structural work proceeded.

A characteristic feature of all measured vertical deformations during the initial periods of concreting was the lifting of the pit bottom, even at loads of from 1 to 1.5 kg per sq. cm, and absence of settlement up to loads from about 2.0 to 3.0 kg per sq. cm. This was particularly noticeable in sections 2, 3 (station III) (Fig. 5 (a)) where settlement began 1.2 years after the start of concreting, when the load of concrete reached almost 3 kg per sq. cm.

Settlement at all sections (averaged for bench marks 1-3 and 7-9) six years after the first concrete was poured, which may be assumed as the time needed for final settlement, is shown in Fig. 5 (b), from which it can be seen that the values change from 13.6 to 25 cm. Maximum settlement may be regarded as settlement during the construction period  $W_{con \text{ in-situ}}$ , the design values being given in Table 2.

The ratio of  $W_{con \text{ in-situ}}$  to  $W_{\infty \text{ II}}$  approaches 0.7, i.e. in this ratio the forecast is very near to natural conditions. Changing of tilting of separate sections with time (Fig. 6) is also corroborated by the law [7] of increase of section tilting observed at other projects in a upstream direction at the water level rose.

In conclusion, it is necessary to note the causes of changes in the values  $W_{\infty \text{ I}}$  and  $W_{\infty \text{ II}}$ , by which final settlement is forecast on the basis of a first approximation.

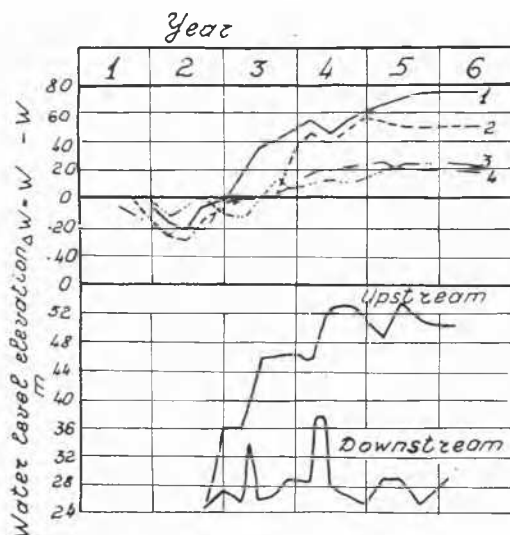


Fig. 6 Tilting of power house. Curves 1-1 tilting related to two bench marks for sections No. 10 and 5. Inclinaisons de l'usine hydroélectrique. Courbes 1-1 des inclinaisons suivant deux repères pour les sections nos 10 et 5.

The authors believe that the chief cause is the excessive increase of dilatation. In practice, when finding  $W_{\infty \text{ I}}$ , it was considered that maximum swelling of the foundation soil occurred between the start of excavation and the first pouring of concrete. However, this assumption was not confirmed. The dilatation process was much slower than assumed, and this was confirmed by the character of the foundation bed deformation during the first period of concrete placing.

## Conclusions

1. Forecast of settlement of hydraulic structures, with a foundation bed consisting mainly of dense clay dilatated soils, is a very complex problem. A factor of considerable importance in such a forecast is the probability of soil dilatation for a significant depth during trench excavation; other important factors include load changes with time, variations of soil properties, both horizontally and vertically, and in-situ observations of settlement of similar structures. False estimates of such factors can lead to forecasts which are completely erroneous.

2. When forecasting settlement of a proposed structure, it was necessary to use new solutions, particularly, when designating the values of the dilatation zones.

3. Observations of movements taken during 6 to 8 years from the beginning of trench excavation and the corroboration of many solutions, as well as the corrections required for some, have shown the necessity of further developing and improving methods of forecasting the settlement of hydraulic structures.

## References

- [1] LEBEDJEV, N. V., UFLJAND, J. C. (1958). Axial-Symmetrical Contact Problem for Elastic Layer. *Applied Mathematics and Mechanics*, Vol. XXII, issue 3.
- [2] YEGOROV, K. E. (1960). Contact Problem for Elastic Layer During Action of Eccentric Vertical Force on Circular Rigid Stamp. *Reports of Academy of Sciences of the U.S.S.R.*, Vol. 133, issue 4.
- [3] BIRMAN, S. E. (1953). On the Settling of a Rigid Stamp on an Elastic Layer Arranged on an Incompressible Foundation Bed. *Reports of the Academy of Sciences of the U.S.S.R.*, Vol. XCIII, No. 5.
- [4] YEGOROV, K. E. (1959). Investigation of Smokestack Foundation Bed Deformations in Layers. *Journal in the U.S.S.R. Foundation Beds, Foundations, Soil Mechanics*, No. 4.
- [5] Standards and Specifications for Designing Natural Foundation Beds of Buildings and Industrial Structures (1955). (*H and Ty* 127-55).
- [6] NICHIPOROVICH, A. A. (1955). Forecast of Settling of Concrete Hydrotechnical Structures of Soft Foundation Beds. *Gidrotekh-Nicheskoje Stroitelstvo*, No. 5.
- [7] NICHIPOROVICH, A. A. (1957). Results of Field Observations on Settlements of Large Hydraulic Structures. *Proceedings of the Fourth International Conference on Soil Mechanics and Foundation Engineering*, p. 387, Vol. I.